International Journal of Engineering Research & Technology (IJERT)
ISSN: 2278-0181
Vol. 2 Issue 3, March - 2013

Parametric Study Of The Material On Mechanical Behavior Of Pressure Vessel

Dr. Mohammad Tariq
Assistant Professor
Mechanical Engineering Department
SSET, SHIATS-Deemed University, Naini, Allahabad,
U.P., India-211016

Er. Mohammed Naeem Mohammed
Midland Refineries Company,
Ministry of Oil, Republic of Iraq

Abstract

The parametric study for pressure vessel which is considered as one of the most significant applications in the daily life under action of the internal pressure that resulting from its operation was implemented. The parametric study of the considered pressure vessel is viewed from two main aspects, material problem and study the effect of structural thickness on the structural behavior of the vessel. A176 carbon steel alloy is used as modeling material. The study of thickness problem is viewed topologically for pressure vessel by varying the vessel thickness gradually to predict the mechanical behavior of the vessel versus thickness variation. The technique was included a finite element modeling of the vessel using high-order isoperimetric plate elements and used to create thick wall cylindrical. The vessel model has been drawn using Ansys Parametric Design Language, in order to implement the parametric study of the problem together with the Ansys package capability.

Keywords- *pressure vessels, stress, strain, ansys, FEA.*

1. Introduction

Two types of analysis are commonly applied to pressure vessels. The most common method is based on a simple mechanics approach and is applicable to "thin wall" pressure vessels which by definition have a ratio of inner radius (r) to wall thickness (t) of $(\frac{r}{t} \geq 10)$. The second method is based on elasticity solution and is always applicable regardless of the (r/t) ratio and can be referred to as the solution for "thick wall" pressure vessels. Both types of analysis are discussed here, although for most engineering applications, the thin wall pressure vessel can be used [22].

Since the vessel is under static equilibrium, it must satisfy Newton's first law of motion. In other words, the stress around the wall must have a net resultant to balance the internal pressure across the cross-section [18].

The internal pressure generates three principal stresses, i.e., a circumferential stress (σ_t), an axial stress (σ_a) and a radial stress (σ_r). As in the case of the cylinder, it has to be examined the tri axial status of stresses, and determine an ideal stress through one of the theories of failure. By setting the ideal stress almost equal to the allowable stress, an equation will be obtained to calculate the minimum required thickness [1].

1.1 Parametric study variables

The pressure vessel's performance depends on many parameters. These parameters can be classified as geometrical parameters, material properties and operating conditions. For each configuration, certain properties of the wall can be calculated. Ranges for each parameter are determined, taking A176 as modeling material reference.

Geometrical parameters are selected to be the wall thickness of the vessel, modeling material of the vessel depending on the application field. It is easily noticeable, that these parameters define the cylindrical vessel with open ends. Hence, different combinations of these variables can be picked to examine the system and obtain relations with the cylindrical wall performance [14].

Solution of the problem is expressed in terms of two parametric functions. The relationship between them suggests that Lame's elastic solution and solution for

perfectly elastic material depend on special choices for these parameters. Both solutions use linear material behavior [4].

1.2 Thick cylinder

Thick walled cylinders subjected to high internal pressure are widely used in various industries. In general, vessels under high pressure require a strict analysis for an optimum design for reliable and secure operational performance. Solutions have been obtained either in analytical form or with numerical implementations.

1.3 Stress analysis in thick cylinder

In general, pressure vessels designed in accordance with the ASME code, section VIII, division 1, are designed by rules and do not require a detailed evaluation of all stresses. It is recognized that high localized and secondary bending stresses may exist but are allowed for by use of a higher safety factor and design rules for details. It is required, however, that all loadings (the forces applied to a vessel or its structural attachments) must be considered.
While the code gives formulas for thickness and stress of basic components, it is up to the designer to select appropriate analytical procedures for determining stress due to other loadings. The designer must also select the most probable combination of simultaneous loads for an economical and safe design. The code establishes allowable stresses and states that the maximum general primary membrane stress must be less than allowable stresses outlined in material sections. Further, it states that the maximum primary membrane stress plus primary bending stress may not exceed 1.5 times the allowable stress of the material sections. These higher allowable stresses clearly indicate that different stress levels for different stress categories are acceptable [8].

2. Finite element model (FEM)

The proposed finite element model and their mesh along global X- and Y-coordinate, location and numbers of the generated nodes and element for the two cases have shown in figs 1.1 and 1.2.
For the case 1, Solid42 plane 4-node elements are used to build this model. The drawn rectangular surface is discretized in to 155 plane elements at size smart 0.1mm. For case 2, Solid82 plane 8-node elements are used to build this model. The drawn rectangular surface is discretized into 429 plane elements at size smart 0.05mm.
ANSYS finite element package can be created to build and analyze of this model, according to the following steps:

The domain of the model is assumed to be rectangular drawn through the plane of global X- and Y- axis; their dimensions are R1 and R2 along global X-axis and depth (height) along global Y-axis for all the four cases taken in this work.

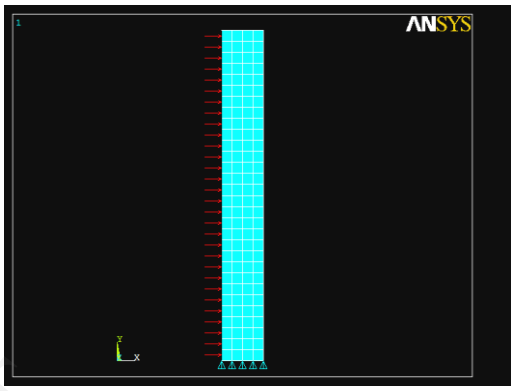

Fig 1.1 Finite element modeling of case 1

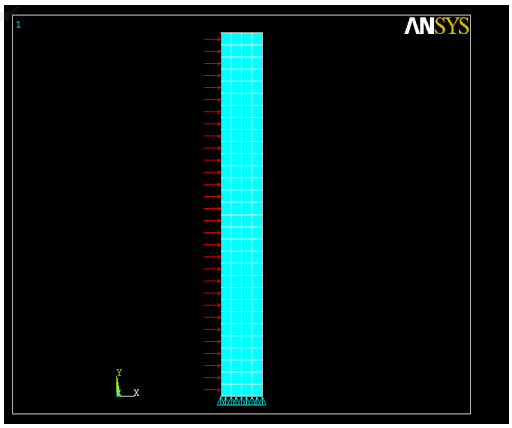

Fig 1.2 Finite element modeling of case 2

2.1 Geometrical shape of case 1 and case 2

Case 1 and 2 having the same geometrical shape and this can be explained as shown in fig (1.3).

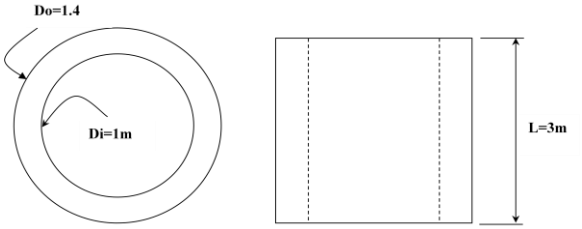

Fig 1.3 geometrical shape of the cylinder

Elements shown in figs. 1.4 and 1.5 have been taken in present work. The stress σ_t constant along the circumference, is exercised on sides A-B and C-D.

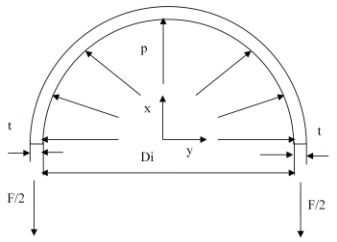

Fig. 1.4 Illustrate the forces in a cylinder

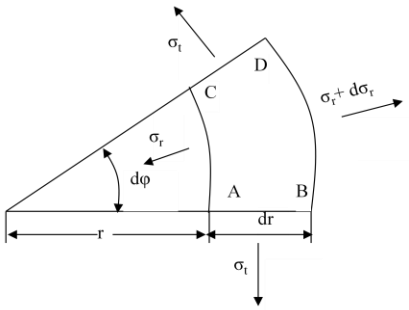

Fig. 1.5 Illustrate the element is subjected to stresses

Forces exerted on sides A-C and B-D are given by

$F_{AC} = \sigma_r r d\varphi$ (1)

$F_{BD} = (\sigma_r + d\sigma_r)(r + dr)d\varphi$ (2)

Finally, on the sides A-B and C-D

$F_{AB} = F_{CD} = \sigma_t dr$ (3)

The resultant based on such two forces in the radial direction is

$F_{BD} = \sigma_t dr d\varphi$ (4)

According to the previous equations, with $d\varphi$ having a nonzero value, will obtain

$$\sigma_t - \sigma_r - r\frac{d\sigma_r}{dr} = 0 \quad (5)$$

This is the equilibrium equation of the cylinder.

As far as the congruence of deformations are concerned, by assuming the circular ring of thickness d_r shown in fig 1.6.

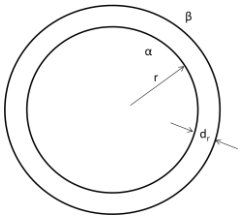

Fig 1.6 the circular ring

Because of the circumferential $\Delta r\alpha$ the radius of circle (α), has an elongation (ε_t). Deformation given by,

$r = \varepsilon_t = \Delta r\alpha$ (6)

The radius of circle (β) in turn has an elongation

$\Delta r\beta = (\varepsilon_t + d\varepsilon_t)(r + dr)$ (7)

To impose congruence, the difference between these two elongations must correspond to the thickness increment of the ring i.e.

$\Delta t = \varepsilon_r dr$ (8)

or

$\Delta r\beta - \Delta r\alpha = \Delta t$ (9)

From (6) and (8)

$$\varepsilon_r + \varepsilon_t - r\frac{d\varepsilon_t}{dr} = 0 \quad (10)$$

Equation (10) is the equation of congruence of the cylinder and,

$$\varepsilon_t = \frac{1}{E}[\sigma_t - \mu(\sigma_t - \sigma_a)] \quad (11)$$

$$\varepsilon_r = \frac{1}{E}[\sigma_r - \mu(\sigma_t - \sigma_a)] \quad (12)$$

$$\varepsilon_a = \frac{1}{E}[\sigma_a - \mu(\sigma_t - \sigma_r)] \quad (13)$$

E is normal modulus of elasticity and μ is the Poisson's ratio.

Principal stresses are calculated by using Lame's equations as follows,

$$\sigma_t = \frac{p}{a^2-1}\left(1 + \frac{r_e^2}{r^2}\right) \quad (14)$$

$$\sigma_r = \frac{p}{a^2-1}\left(1 - \frac{r_e^2}{r^2}\right) \quad (15)$$

$$\sigma_a = \frac{p}{a^2-1} \quad (16)$$

2.2 Displacement calculation

The displacement in the thick wall cylinder is given by,

$$u_r = \frac{1-\mu}{E}\left[\frac{p_i r_i^2 - p_o r_o^2}{r_o^2 - r_i^2}\right] r + \frac{(1+\mu)}{E}\frac{(p_i - p_o) r_i^2 r_o^2}{r_o^2 - r_i^2}\frac{1}{r} \quad (17)$$

2.3 Coordinates systems

There are three types of coordinates systems used in above finite element models, these are:

1- The global coordinates system.
2- The nodal coordinates system.
3- The element coordinates system.

2.4 Stress-Strain Relationship

The axi-symmetric stress-strain relations in cylindrical coordinates aligned with principle material directions is given by,

$$\begin{Bmatrix}\sigma_r\\ \sigma_\theta\\ \tau_{r\theta}\end{Bmatrix}=\frac{E(1-\nu)}{(1+\nu)(1-2\nu)}\begin{bmatrix}(1-\nu) & \nu & 0\\ \nu & (1-\nu) & 0\\ 0 & 0 & \frac{(1-2\nu)}{2}\end{bmatrix}\begin{Bmatrix}\varepsilon_r\\ \varepsilon_\theta\\ \gamma_{r\theta}\end{Bmatrix} \quad (18)$$

where σ_r is the radial stress, σ_θ is the tangential stress, $\tau_{r\theta}$ is the shear stress, ν is the Poisson's ratio and E is the modules of elasticity.

2.5 Element Parameters

All above finite element models have been created using linear four-node quadrilateral plane and eight-node elements. This type of element is used for idealization of pressure vessel (Thick cylinder) in 2D. In this section, the parameters that are concerned with the selected element are discussed. These parameters are basically included the element property parameters and the material properties at each node of the structure pressure vessel. The material properties for whole vessel are specified as isotropic material. The element degrees of freedom are assigned at each node along the element coordinate system. The displacement at each node is given by,

$$\begin{Bmatrix}u(\xi,n)\\ v(\xi,n)\end{Bmatrix}=\sum_{i=1}^{k}N_i(\xi,n)\begin{Bmatrix}u_i\\ v_i\end{Bmatrix} \quad (19)$$

k is 4 for plane 42 four node and 8 for plane 82 eight node, N_i is the shape function, u_i and v_i are global nodal displacements, ξ and η are local coordinate for elements. It is obvious that each node has two degree of freedom, and then the element is of eight degrees of freedom in plane 42 and sixteen degrees of freedom in plane 82. Not all but some of the element degrees of freedom are considered at each of the finite element models, depending upon the function (boundary conditions) of that model.

2.5.1 Linear four- node quadrilateral plane42

The shape function for plane 42 four node is represented as,

$$\left.\begin{aligned}N_1(\xi,n)&=\tfrac{1}{4}(1-\xi)(1-\eta)\\ N_2(\xi,n)&=\tfrac{1}{4}(1+\xi)(1-\eta)\\ N_3(\xi,n)&=\tfrac{1}{4}(1+\xi)(1+\eta)\\ N_4(\xi,n)&=\tfrac{1}{4}(1-\xi)(1+\eta)\end{aligned}\right\} \quad (20)$$

where ξ and η are local coordinate for elements.
For this element the matrix [B] is given by,

$$[B]=\frac{1}{|J|}[B_1B_2B_3B_4] \quad (21)$$

$[B_i]$ is given by,

$$[B_i]=\begin{bmatrix}a\frac{\partial N_i}{\partial\xi}-b\frac{\partial N_i}{\partial\eta} & 0\\ 0 & c\frac{\partial N_i}{\partial\eta}-d\frac{\partial N_i}{\partial\xi}\\ c\frac{\partial N_i}{\partial\eta}-d\frac{\partial N_i}{\partial\xi} & a\frac{\partial N_i}{\partial\xi}-b\frac{\partial N_i}{\partial\eta}\end{bmatrix} \quad (22)$$

Where;

$$\left.\begin{aligned}a&=\tfrac{1}{4}[y_1(\xi-1)+y_2(-1-\xi)+y_3(1+\xi)+y_4(1-\xi)]\\ b&=\tfrac{1}{4}[y_1(\eta-1)+y_2(1-\eta)+y_3(1+\eta)+y_4(-1-\eta)]\\ c&=\tfrac{1}{4}[x_1(\eta-1)+x_2(1-\eta)+x_3(1+\eta)+x_4(-1-\eta)]\\ d&=\tfrac{1}{4}[x_1(\xi-1)+x_2(-1-\xi)+x_3(1+\xi)+x_4(1-\xi)]\end{aligned}\right\} \quad (23)$$

Since the shape functions N are functions of the local coordinates rather than Cartesian coordinates, a relationship needs to be established between the derivatives in the two coordinates systems. By using the chain rule, the partial differential relation can be expressed in matrix form as,

$$\begin{bmatrix}\frac{\partial N_i}{\partial\xi}\\ \frac{\partial N_i}{\partial\eta}\end{bmatrix}=\begin{bmatrix}\frac{\partial x}{\partial\xi} & \frac{\partial y}{\partial\xi}\\ \frac{\partial x}{\partial\eta} & \frac{\partial y}{\partial\eta}\end{bmatrix}\begin{bmatrix}\frac{\partial N_i}{\partial x}\\ \frac{\partial N_i}{\partial y}\end{bmatrix} \quad (24)$$

where [J] is the Jacobian matrix and the elements of this matrix can be obtained by differentiating the following equations;

$$\left.\begin{aligned}x(\xi,\eta)&=\sum_{i=1}^{4}N_i(\xi,\eta)x_i\\ y(\xi,\eta)&=\sum_{i=1}^{4}N_i(\xi,\eta)y_i\end{aligned}\right\} \quad (25)$$

$$[J]=\begin{bmatrix}\sum_{i=1}^{4}\frac{\partial N_i}{\partial\xi}x_i & \sum_{i=1}^{4}\frac{\partial N_i}{\partial\xi}y_i\\ \sum_{i=1}^{4}\frac{\partial N_i}{\partial\eta}x_i & \sum_{i=1}^{4}\frac{\partial N_i}{\partial\eta}y_i\end{bmatrix} \quad (26)$$

Then, the derivatives of the shape function with respect to Cartesian coordinates can be given as:

$$\begin{bmatrix}\frac{\partial N_i}{\partial x}\\ \frac{\partial N_i}{\partial y}\end{bmatrix}=[J]^{-1}\begin{bmatrix}\frac{\partial N_i}{\partial\xi}\\ \frac{\partial N_i}{\partial\eta}\end{bmatrix} \quad (27)$$

Where $[J]^{-1}$is the inverse of Jacobian matrix given by,

$$[J]^{-1}=\begin{bmatrix}\frac{\partial\xi}{\partial x} & \frac{\partial\eta}{\partial x}\\ \frac{\partial\xi}{\partial y} & \frac{\partial\eta}{\partial y}\end{bmatrix} \quad (28)$$

The determinant |J| is given by,

$$|J| = \frac{1}{8}[x_1\ x_2\ x_3\ x_4\ ] = \begin{bmatrix} 0 & 1-\eta & \eta-\xi & \xi-1 \\ \eta-1 & 0 & 1+\xi & -\eta-\xi \\ \xi-\eta & -1-\xi & 0 & 1+\eta \\ 1-\xi & \eta+\xi & -1-\eta & 0 \end{bmatrix} \quad (29)$$

For the case of plane stress, matrix [D] is given by,

$$[D] = \frac{E}{1-\nu^2}\begin{bmatrix} 1 & \nu & 0 \\ \nu & \nu & 0 \\ 0 & 0 & \frac{1-\nu}{2} \end{bmatrix} \quad (30)$$

For the case of plane strain, matrix [D] is given by,

$$[D] = \frac{E}{(1+\nu)(1-2\nu)}\begin{bmatrix} 1-\nu & \nu & 0 \\ \nu & 1-\nu & 0 \\ 0 & 0 & \frac{1-2\nu}{2} \end{bmatrix} \quad (31)$$

2.5.2 Quadratic eight-node quadrilateral plane 82

The shape functions are;

$$\left.\begin{aligned} N_1 &= \tfrac{1}{4}(1-\xi)(1-\eta)(-\xi-\eta-1) \\ N_2 &= \tfrac{1}{4}(1+\xi)(1-\eta)(\xi-\eta-1) \\ N_3 &= (1+\xi)(1+\eta)(\xi+\eta-1) \\ N_4 &= \tfrac{1}{4}(1-\xi)(1+\eta)(-\xi+\eta-1) \\ N_5 &= \tfrac{1}{4}(1-\eta)(1+\xi)(1-\xi) \\ N_6 &= \tfrac{1}{4}(1+\eta)(1+\xi)(1-\eta) \\ N_7 &= \tfrac{1}{4}(1+\eta)(1+\xi)(1-\xi) \\ N_8 &= \tfrac{1}{4}(1-\xi)(1+\eta)(1-\eta) \end{aligned}\right\} \quad (32)$$

The Jacobian Matrix for this element is given by,

$$[J] = \begin{bmatrix} \frac{\partial x}{\partial \xi} & \frac{\partial y}{\partial \xi} \\ \frac{\partial x}{\partial \eta} & \frac{\partial y}{\partial \eta} \end{bmatrix} \quad (33)$$

Where x and y are given by:

$$\left.\begin{aligned} N_1x_1 + N_2x_2 + N_3x_3 + N_4x_4 + N_5x_5 + N_6x_6 + N_7x_7 + N_8x_8 \\ N_1y_1 + N_2y_2 + N_3y_3 + N_4y_4 + N_5y_5 + N_6y_6 + N_7y_7 + N_8y_8 \end{aligned}\right\} \quad (34)$$

The matrix [B] for this element is given as follows:

$$[B] = [D][N] \quad (35)$$

$$[D] = \frac{1}{|J|}\begin{bmatrix} \frac{\partial y}{\partial \eta}\frac{\partial ()}{\partial \xi} - \frac{\partial y}{\partial \xi}\frac{\partial ()}{\partial \eta} & 0 \\ 0 & \frac{\partial x}{\partial \xi}\frac{\partial ()}{\partial \eta} - \frac{\partial x}{\partial \eta}\frac{\partial ()}{\partial \xi} \\ \frac{\partial x}{\partial \xi}\frac{\partial ()}{\partial \eta} - \frac{\partial x}{\partial \eta}\frac{\partial ()}{\partial \xi} & \frac{\partial y}{\partial \eta}\frac{\partial ()}{\partial \xi} - \frac{\partial y}{\partial \xi}\frac{\partial ()}{\partial \eta} \end{bmatrix} \quad (36)$$

$$[N] = \begin{bmatrix} N_1\ 0 + N_2\ 0 + N_3\ 0 + N_4\ 0 + N_5\ 0 + N_6\ 0 + N_7\ 0 + N_8\ 0 \\ 0\ N_1 + 0\ N_2 + 0\ N_3 + 0\ N_4 + 0\ N_5 + 0\ N_6 + 0\ N_7 + 0\ N_8 \end{bmatrix} \quad (37)$$

2.6 Strain–displacement relationship

The geometrical nonlinearity is not considered in the present work hence, the engineering components of strain can be expressed in terms of first partial derivatives of the displacement components. Therefore, the linear strain–displacement relation at any point on element and for two degrees of freedom per node can be written as;

$$\varepsilon_r = \frac{\partial u}{\partial r},\ \varepsilon_\theta = \frac{u}{r} \text{ and } \varepsilon_z = \frac{\partial w}{\partial z}.$$

$$\gamma_{r\theta} = \frac{\partial u}{\partial z} + \frac{\partial w}{\partial r} \quad (38)$$

2.7 Boundary conditions

The specify boundary conditions include the constraint and free state of the degrees of freedom at each node in the finite element models. The state of the degree of freedom is constrained or free, depending upon the model itself. From the all model to the eight model, the cylindrical structural model is fixed from the bottom joining nodes thus all these nodes are constraint in all their degrees of freedom. Thus in the corresponding finite element model, the nodes that are located on the end of cylinder are of constrained degrees of freedom, while all other nodes above the bottom are free of degrees of freedom as shown in fig 2.1.

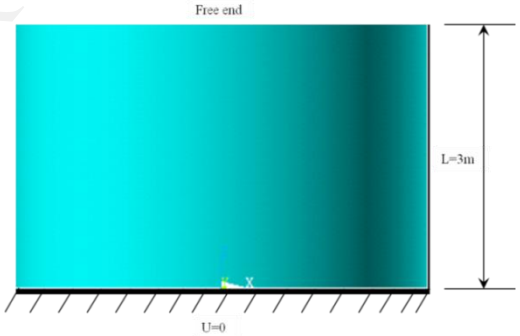

Figure 2.1 boundary condition of the cylinder

2.8 Static analysis

Static analysis is achieved on each of the finite element models for each function with their corresponding boundary conditions and load sets. Static analysis solution has been included the calculation of the effects of the applied static distributed loads on each model for each function with the corresponding boundary conditions. These effects included displacements, strains, and stresses that are induced in the structure due to the applied

loads. The static analysis is governed by the following equilibrium equations (in matrix notation):

$[K].\{u\} = \{F\}$ (39)

where [K] the assembled stiffness matrix is given by,

$[K] = \sum_{e=1}^{N} [K]^e$ (40)

ANSYS solve the above equilibrium equations to obtain the following results:

a) Displacements of each node along their free degrees of freedom.
b) Strains and stresses at each element along element coordinate axis.
c) Principle stresses and strain values and directions with respect to the element coordinates axis at each element.
d) Von-Mises stresses and the maximum shear stresses.

2.9 Material modeling

The modeling material for pressure vessel is selected from carbon steel alloys scheduled in table (1).

Table (1) Properties of modeling material

Material	E (Gpa)	σ_{yield} (Mpa)	$\sigma_{ultimate}$ (Mpa)	ρ (kg/m^3)	ν
Carbon steel (A176)	206.83	205	415	7800	0.3

2.10 Specification of cases studies

Table (2) State of cases

Case	R1(m)	R2(m)	L (m)	Material	Type of element	Pressure (Mpa)	Thickness (m)
1	1	1.4	3	A176	Solid 42	5	0.4
2	1	1.4	3	A176	Solid 82	5	0.4

2.11 Assumptions

1- Internal pressure applied to inner area.
2- Fixed base of cylinder (Ux, Uy) = 0.
3- Modeling element restricted to solid element only.
4- Using Von-mises criterion in the estimation of stress level of elements.
5- Modeling material restricted to isotropic material only.
6- No bending, no torsion, no external pressure and no thermal effect.
7- Axisymmetric pressure vessel is considered in present work.
8- Open end thick cylinder.

3 Results

3.1 Case study

As parametric study, the pressure vessel problem is based on geometrical investigation. The implementation of comparative study between two element types solid42 and solid82, by selecting the most applicable materials used for manufacturing of pressure vessels (A176 austenitic stainless steel type 410S- UNS- S41008).

3.1.1 Detail of case studies

The present study is restricted to take 2-case studies to illustrate the difference among them by showing the contour plots that captured immediately from ANSYS program.

3.1.2 Comparison with maximum stress

Table (3) Maximum stress of cases

Cases	Stress(Mpa)		
	(σ_r)	(σ_θ)	$(\sigma_{von-mises})$
Case 1	-5.0271	15.541	18.518
Case 2	-4.9558	15.372	18.359

3.1.3 Comparison with maximum displacement

Table (4) Maximum displacement of cases

Cases	Displacement (m)	
	(U_r) (m)	$(U_{absolute})$ (m)
Case 1	82407E-9	93831E-9
Case 2	81790E-9	93510E-9

3.1.4 Comparison with maximum strain

Table (5) Maximum strain of cases

Cases	Strain (max)			
	(ε_r) (m)	(ε_θ) (m)	(ε_z) (m)	$(\varepsilon_{von-mises})$
Case 1	-47316E-10	81962E-10	-1604E-10	11639E-9
Case 2	-4625E-10	81512E-10	-15109E-10	11539E-9

3.1.5 Comparison at A176 and element at thickness 0.4m

Table (6) Comparison between case 1 and case 2

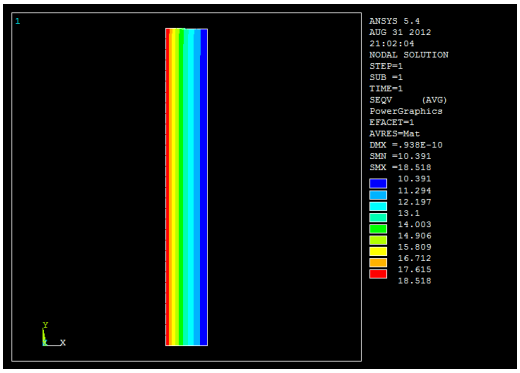

(a) Von-Mises stress distribution in (pa) case 1

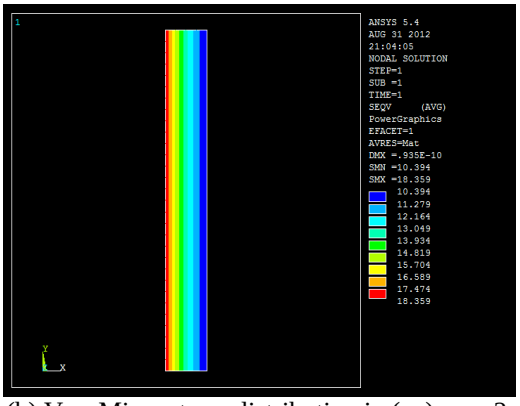

(b) Von-Mises stress distribution in (pa) case 2

Fig. 3.1 Illustrative contours for nodal Von-Mises stress distribution

3.2 Parametric study: Case 1 and Case 2

3.2.1 Stress investigation

Through the investigation of stress for case 1, it is noted that the stress Von-Mises having the maximum value at node 36 which is equal to 18.518 Mpa as compared to case 2 as mentioned in table (3). It is noted that $(\sigma_{von-mises})_{max}$ for case 2 having value 18.359 Mpa at node 1 which is less than that obtained for case 1 due to different in type of element used as shown in figures (3.1 a, b).

Mechanical behavior	Case1– solid42	Case 2-solid 82
$(\sigma_r)_{max}$ (Mpa)	-5.0271	-4.9558
$(\sigma_\theta)_{max}$ (Mpa)	15.541	15.372
$(\sigma_{von-mises})_{max}$ (Mpa)	18.518	18.359
$(U_r)_{max}$ (mm)	82407E-9	81790E-9
$(U_{absolute})_{max}$ (mm)	93831E-9	93510E-9
$(\varepsilon_r)_{max}$	-47316E-9	-46250E-9
$(\varepsilon_\theta)_{max}$	81962E-9	81512E-9
$(\varepsilon_z)_{max}$	-16040E-9	-15109E-9
$(\varepsilon_{von-mises})_{max}$	116390E-9	115390E-9

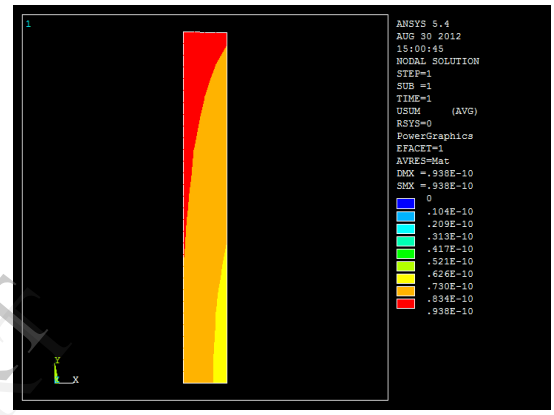

(a) Absolute displacement distribution (case 1)

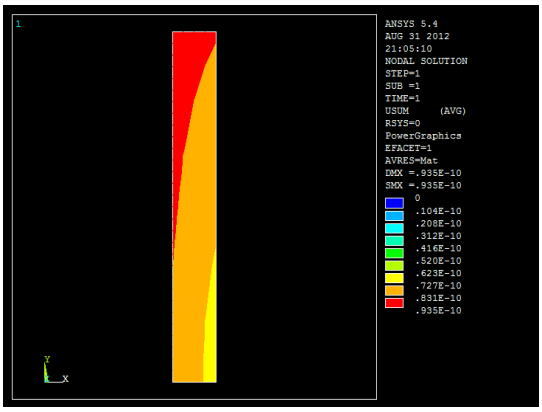

(b) Absolute displacement distribution (case 2)

Figure 3.2 Illustrative contours for nodal absolute displacement distribution

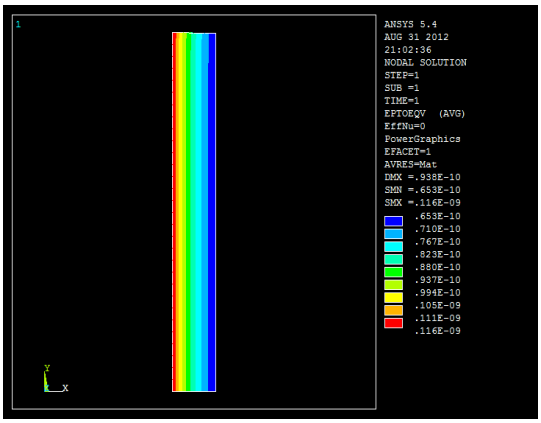

(a) Von-Mises strain distribution case (1)

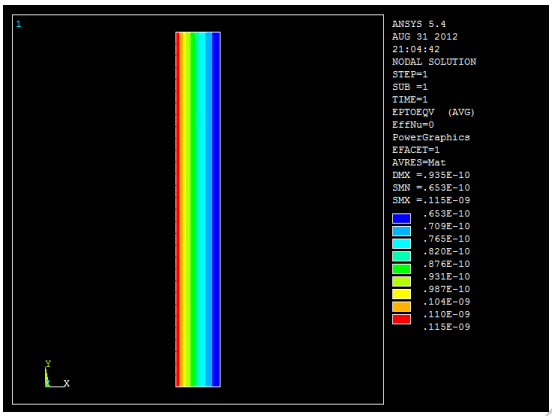

(b) Von-Mises strain distribution case (2)

Fig 3.2 Illustrative contours for nodal Von-Mises strain distribution

3.2.2 Displacement investigation

Through the investigation of displacement for case 1, it is noted that the displacement having the maximum value at node 36 which is equal to 93831E-9 (m) as compared to case 2 as listed in table (4). It is noted that $(U_{absolute})_{max}$ for case 2 having value 93510E-9 (m) at node 70 which is less than that obtained for case1 due to different in type of element used as shown in figure (3.2a, b).

3.2.3 Strain investigation

Through the investigation of strain for case 1, it is noted that the strain having the maximum value at node 36 which is equal to 116390E-9 as compared to case 2 as shown in table (5). It is noted that $(\varepsilon_{von-mises})_{max}$ for case 2 having value 115390E-9 at node 1 which is less than that obtained for case1 due to difference in type of element used as shown in figure (3.3 a, b).

3.3 Analytical calculation

For a thick wall cylinder with the parameters as shown in table (2) the stresses, strains and displacement calculated by the model using equations (11) through (17) are given for all the cases and the results were compared with the numerically analyzed by finite element method.

The results obtained have been plotted in "Origin 6.1" for given cases. Two different methods have been applied for the calculation of stresses and strains at internal pressure (5MPa).

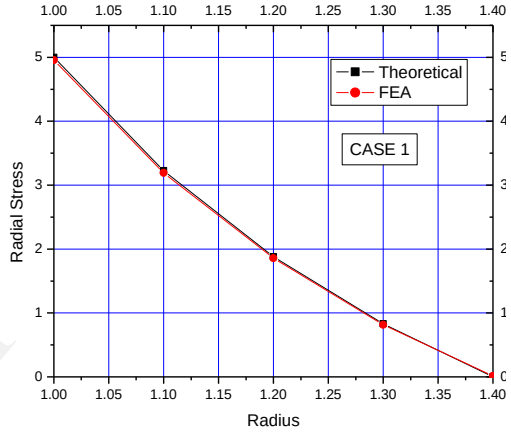

Fig (3.1) Radial stress vs. thickness of cylinder

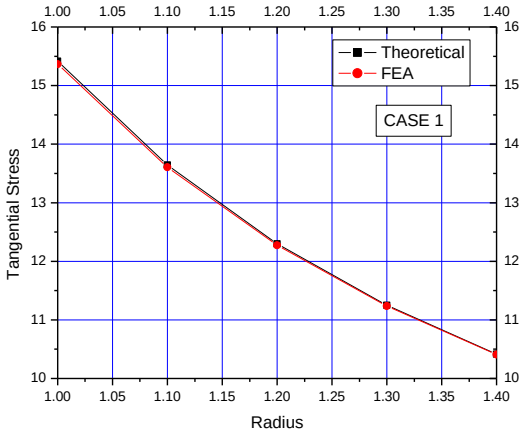

Fig (3.2) Tangential stress vs. thickness of cylinder

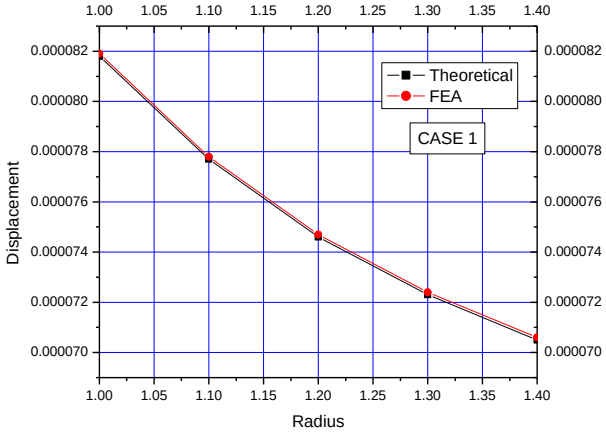

Fig (3.3) Displacement vs. thickness of cylinder

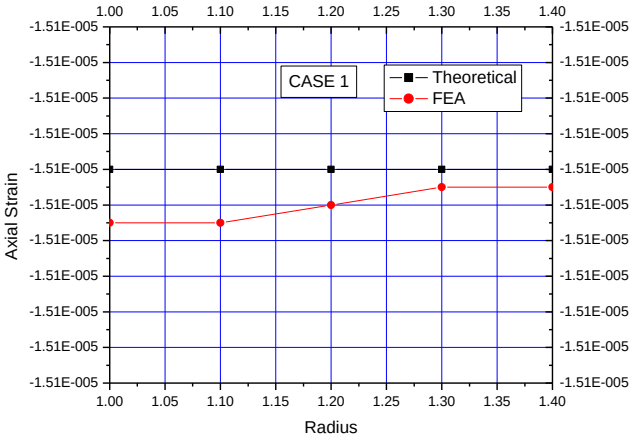

Fig (3.6) Axial strain vs. thickness of cylinder

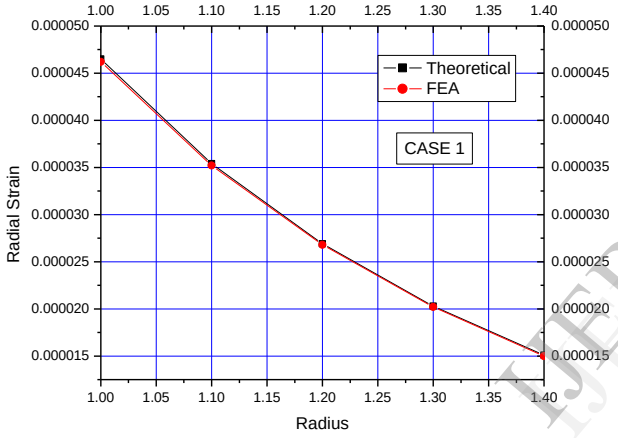

Fig (3.4) Radial strain vs. thickness of cylinder

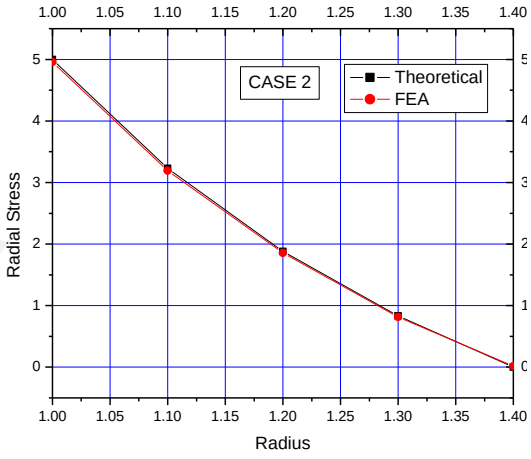

Fig (3.7) Radial stress vs. thickness of cylinder

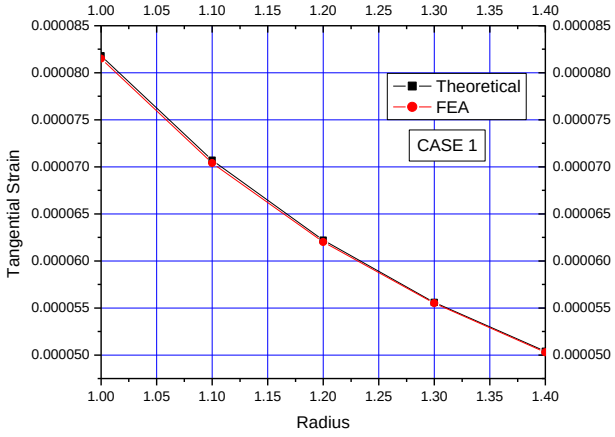

Fig (3.5) Tangential strain vs. thickness of cylinder

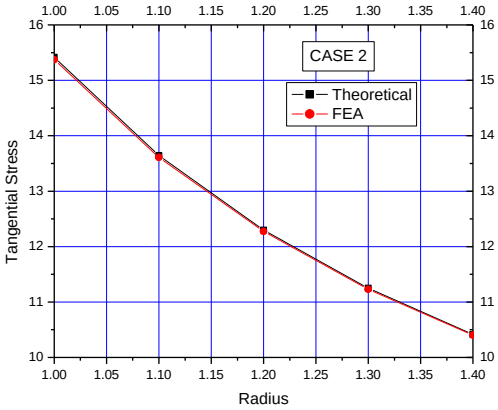

Fig (3.8) Tangential stress vs. thickness of cylinder

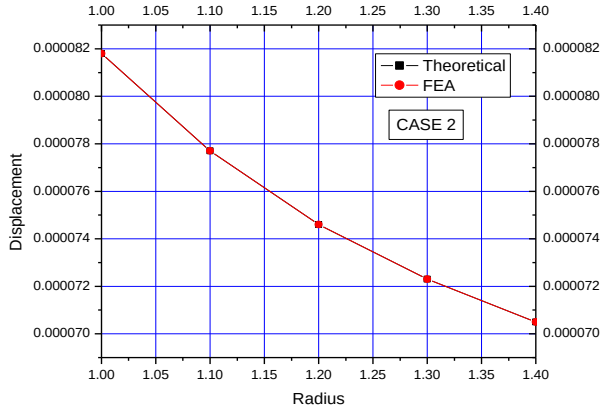

Fig (3.9) Displacement vs. thickness of cylinder

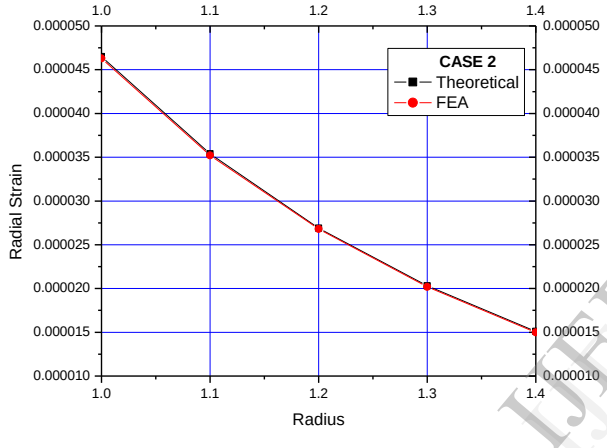

Fig (3.10) Radial strain vs. thickness of cylinder

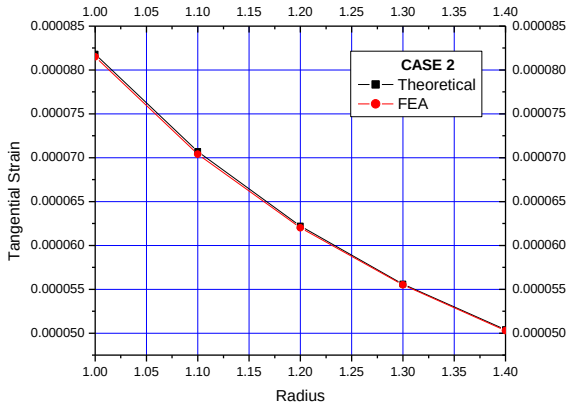

Fig (3.11) Tangential strain vs. thickness of cylinder

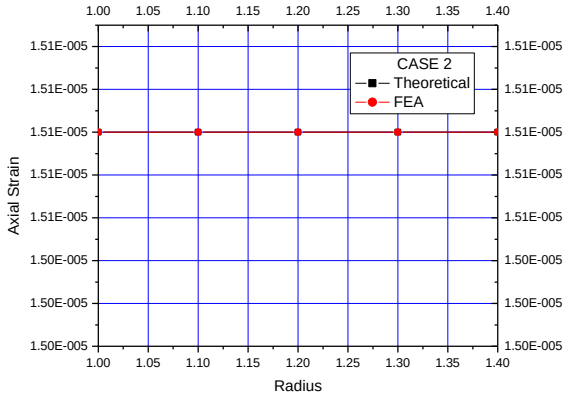

Fig (3.12) Axial strain vs. thickness of cylinder

3.4 Comparison of the analytical and numerical results

The results of the stress, strain and displacement distribution obtained from analytical (thick-walled cylinder theory, Lame's equations) and numerical techniques (FEA) were compared with respect to radial stress versus radius at internal pressure. The stress obtained from the two methods change linearly and gradual decrease from inner radius to outer radius with the applied internal pressure along the wall thickness of the cylinder is shown in figs (3.1) and (3.7). The highest radial stress is found at inner radius i.e. at the inner wall of the cylinder. It can be seen that the results obtained from the two techniques are in good agreement.

The tangential stress obtained from the analytical and FEA methods change linearly with the applied internal pressure. In figs (3.2) and (3.8), gradual decrease in the tangential stress from inner to outer radius has been shown. The highest tangential (hoop) stress is found at the inner radius i.e. at the inner wall of the cylinder. It can be seen that the results obtained from the two techniques are in good agreement.

The displacement distribution obtained from two methods shows a gradual decrease. The highest displacement is found at inner radius as shown in figures (3.3) and (3.9). It can be seen that the results obtained from the two techniques are in good agreement.

The radial strain obtained from two methods change linearly with the applied internal pressure. The highest radial strain is found at inner radius and decreases gradually to outer radius as shown in figures (3.4) and (3.10). It can be seen that the results

obtained from the two techniques are in good agreement.

The tangential strain obtained from two methods change linearly with the applied internal pressure as shown in figures (3.5) and (3.11). It can be seen that the results obtained from the two techniques are in good agreement.

The axial strain obtained from two methods is remained constant through wall thickness as shown in figures (3.6) and (3.12). The axial strain in FEA change through wall thickness is highest at inner radius and decreases to outer radius and in theoretical method the axial strain remain constant through wall thickness. It can be seen that the results obtained from the two techniques are in good agreement.

List of symbols

F	-	Force
P	-	Pressure
D	-	Diameter
t	-	Thickness
σ_r	-	Radial Stress
σ_θ	-	Tangential Stress
σ_a	-	Axial Stress
β	-	Radians of circle
ε_r	-	Radial Elongation
$\varepsilon_\theta/\varepsilon_t$	-	Tangential Elongation
ε_z	-	Axial Elongation
E	-	Modulus of elasticity
μ	-	Poisson's ratio
u_r	-	Radial displacement
Ux, Uy	-	Nodal displacement
Sx, Sy	-	Nodal stress
x, y	-	Global coordinates
R1	-	Inner radius of model
R2	-	outer radius of model
$\Upsilon_{r\theta}$	-	Shear Strain
$\tau_{r\theta}$	-	Shear Stress
Ni	-	Shape function
ξ, η	-	Local Coordinate
[B]	-	Strain matrix
J	-	Jacobian
[D]	-	Constitutive matrix
π	-	Potential energies
SE	-	Strain energy
WF	-	Work done
W_F	-	External work
[K]	-	Stiffness matrix
[F]	-	External applied force matrix
$\lvert J \rvert$	-	Determinate at the jacobian matrix
L	-	Length
σ_t	-	Hoop stress
σ_a	-	Longitudinal stress

References

[1] Donatello, Annaratone, "Pressure vessel design", ISBN-10 3-540-49142-2 springer berlin heidelberg new york, springer-verlag berlin heidelberg, (2007).

[2] Timoshenko, S., S. Woinowsky**,** "Theory of plates and shells", Mcgraw-hill book company, 2nd Edition, (2008).

[3] J. Shigley & Charles M., "Pressure cylinder", mechanical engineering design 5th ed. Mcgraw hill, New York, (2002).

[4] Zhao, W., Seshadri, R., & Dubey, R. N., "On thick-wall cylinder under internal pressure", Journal of pressure vessel technology, Vol.125/267, (2003).

[5] Yi, W., Basavaraju, C., "Cylindrical shells under partially distributed radial loading", transactions of the ASME, vol.118, pp. 104 (1996).

[6] Heckman David, "Finite element analysis of pressure Vessels" university of California, (1998).

[7] Roylance, David, "Pressure vessels" Department of materials science and engineering, Massachusetts institute of technology Cambridge, MA 02139, (2001).

[8] R. Moss, Dennis, "Pressure vessel design manual" third edition**,** gulf professional publishing, (2004).

[9] Yosibash, zohar et al., "Axisymmetric pressure boundary loading for finite deformation analysis using p-FEM" Elsevier vol.196 , no. 7, p.p. 1261-1277.

[10] Carbonari, R. C., Munoz-Rojas, P. A., "Design of pressure vessels using shape optimization: An integrated approach" International journal of pressure vessels and piping vol. 88 pp 198-212, (2007).

[11] Z. Kabir, Mohammad**,** "Finite element analysis of composite pressure vessels with a

load sharing metallic liner" Composite structures vol. 49 pp 247-255, (2000).
[12] Kelly, Piaras, "Solid mechanics part 1 an introduction to solid mechanics" fourth edition, (2008).
[13] Leisis, V. et al. "Prediction of the strength and fracture of the fuel storage tank", ISSN 1392-1207. Mechanika Nr. 4 (72), (2008).
[14] BSME, Ilgaz Cumalioglu, "Modeling and simulation of a high pressure hydrogen storage tank with dynamic wall", M.Sc. thesis, Faculty of Texas tech university, (2005).
[15] Hojjati, M. H. & Hassani, A., "Theoretical and finite-element modeling of autofrottage process in strain-hardening thick walled cylinders" International journal of pressure vessels and piping vol. 84 pp 310–319, (2007).
[16] Amin, M. & Ahmed S., "Finite element analysis of pressure vessel with flat metal ribbon wound construction under the effect of changing helical winding angle", Journal of space technology, Vol 1, No.1, (2011).
[17] Kaminski, Clemens, "Stress analysis & pressure vessels", university of Cambridge, (2005).
[18] Rangari, D. L. et al., "Finite element analysis of LPG gas cylinder", International journal of applied research in mechanical engineering (IJARME) ISSN:2231–5950, Volume-2, Issue-1, (2012).
[19] You, L. H., et al., "Elastic analysis of internally pressurized thick-walled spherical pressure vessels of functionally graded materials", International journal of pressure vessels and piping, vol. 82 pp 347–354, (2005).
[20] Coman O., et al., "Accident pressure analysis for a reinforced concrete containment with steel liner", Transactions of the 17th international conference on structural mechanics in reactor technology (SMIRT 17) Prague, Czech Republic, (2003).
[21] R. Liu, G., & S. Quek, S., "The finite element method: A practical course" Elsevier science Ltd, (2003).
[22] Carbonari, R. C., et al. "Design of pressure vessels using shape optimization: An integrated approach", International journal of pressure vessels and piping, Vol. 88, Issues 5–7, Pages 198–212, (2011).